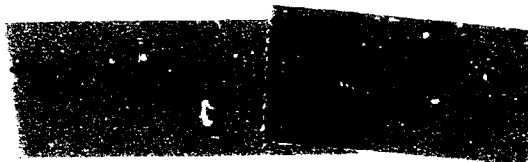


COMITETUL DE STAT PENTRU ENERGIA NUCLEARA
INSTITUTUL DE FIZICA ATOMICA

FN-43-1973



INSTRUMENTAL WIDTHS AND INTENSITIES
IN NEUTRON CRYSTAL DIFFRACTOMETRY

B. GRABCEV

Bucharest - ROMANIA

We regret that some of the pages in the microfiche copy of this report may not be up to the proper legibility standards, even though the best possible copy was used for preparing the master fiche.

**EXPERIMENTAL VALUES AND INTERPRETATION
IN NEUTRON CRYSTAL DIFFRACTION**

B. Grabcev

Institute for Atomic Physics, Bucharest, P.O.B. 327

C O N T E N T S

I. Quasielastic resolution function of a two-axis spectrometer	1
II. Analysis of the elastic coherent neutron scattering in crystals	27

I. QUASIELASTIC RESOLUTION FUNCTION OF A TWO-AXIS SPECTROMETER

The amplitude and the shape of the quasi-elastic resolution function of a neutron two-axis spectrometer are calculated in the Gaussian approximation. Special attention is given to the explicitness of the formulae as well as to their absolute character, avoiding any unknown proportionality factors.

1. Introduction

In an experiment, analysing the angular distribution of the scattered neutrons, carried on with a crystal diffractometer (two-axis spectrometer), the finite collimations, the monochromator mosaic structure and the beam-path configuration influence both the counting rate and the experimental line width. This influence should be quantitatively described by an instrumental function, the so called resolution function.

The knowledge of the resolution function enables the choice of advantageous experimental conditions as well as the correct interpretation of experimental data. That is why a considerable attention has been paid to the problem of deriving analytical formulae expressing the dependence of the diffractometer resolution function on all experimental factors. However, almost all the papers which have been published so far on this subject deal with elastic scattering experiments, their principal aim being the determination of Bragg

of the relative intensities for various scattering procedures (Gasper, 1957; Cooper & Ricci, 1951, 1953; Torgazzi & Ricci, 1952; Gabor, 1954; Cooper & Nathans, 1953 a, 1953 b; Cooper, 1957; Collins, 1957) the case of an inelastic cross-section is especially well covered by Torgazzi and coworkers (1952).

In the present paper we pay both the aptitude and the range of the resolution function of a neutron optical diffractometer the solution of the dispersion approximation (1956). There is assumed the energy resolution function of the collimator as well as the resolution function of the detector (with the sinc-like functions). The first part of the present quasielastic scattering process, considered in the present paper, is the two-axis analysis (represented by the traditional experimental method). Special attention is given to the generality of the formulae as well as to their absolute character, avoiding any unknown proportionality factors.

Although the resolution function of the diffractometer may be considered simply as a special case of the resolution function determined by a three-axis spectrometer (Cooper & Nathans, 1957; Grabcev, 1953 a, 1953 b) it is treated here independently in order to avoid the necessity of knowing details concerning the three-axis spectroscopy and, on the other hand, to outline the features of two-axis analysis.

Even if the two-axis spectrometer performs no energy analysis there exists an explicit dependence of its resolution function on energy transfers, which must be taken into account in quasielastic experiments.

Using for the definition of the resolution function the same variables which express the scattering cross-sections, two cases are separately considered :

1) The sample is an anisotropic system (single crystal or magnetized sample, e.g.). The resolution function is expressed with res -

to four variables: the three components of momentum transfer and the energy transfer.

(ii) The sample is an isotropic system (polycrystal or liquid, etc.) In this case the resolution function depends only on the magnitudes of momentum transfer and on the energy transfer.

1. General expression of the counting rate

Using, generally, the Cooper & Nathans (1967) notation, recorded in Table 1, the counting rate, for a diffractometer setting defined by \vec{k}_I and \vec{k}_F , may be written as:

$$C(\vec{k}_I, \vec{k}_F) = N \int_{\vec{k}_I} \Phi(\vec{k}_I) T_M(\vec{k}_I, \vec{k}_I) \frac{d\sigma}{d\vec{k}_I} T_A(\vec{k}_F) \xi(k_F) d\vec{k}_I d\vec{k}_F \quad (1)$$

where:

N is the number of atoms (or unit cells) in the sample,

$\Phi(\vec{k})$ is the \vec{k} -density of the neutron source flux:

$$\Phi(\vec{k}) = \frac{\Phi_0}{2\pi} \frac{k}{k_T} e^{-k^2/k_T^2};$$

Φ_0 is the total thermal flux, and:

$$k_T = \sqrt{2mk_B T/h^2}$$

$T_M(\vec{k}_I, \vec{k}_I)$ is the transmission function of the monochromator system for \vec{k}_I neutrons when the \vec{k}_I neutrons are preferentially transmitted,

$\frac{d\sigma}{d\vec{k}_I}$ is the sample cross section per atom (or unit cell) and volume unit in \vec{k}_I space,

$T_A(\vec{k}_F)$ is the transmission function of the analysing system,

$\xi(k_F)$ is the detector counting efficiency for k_F neutrons.

TABLE I

\vec{k}_i	Any incident wave vector
\vec{k}_i^*	The most probable \vec{k}_i .
\vec{k}_f	Any scattered wave vector
\vec{k}_f^*	The most probable \vec{k}_f
α_j	Horizontal collimation angle
β_j	Vertical collimation angle
δ_j	Horizontal divergence angle
ϵ_j	Vertical divergence angle
$j=0$	In-pile region
$j=1$	Monochromator to sample region
$j=2$	Sample to counter region
Δ_M	Horizontal mosaic spread of the monochromator crystal
Γ_M	Vertical mosaic spread of the monochromator crystal
ϕ	Angle between \vec{I} -axis and \vec{k}_i
θ_M	Bragg angle for \vec{k}_i^* neutrons

As it was already pointed out, in the present calculations only elastic or at the most quasielastic scattering processes are considered. In fig. 1 there is shown a vector diagram in the reciprocal space corresponding to the most probable scattering process. The \vec{k} -axis of the rectangular reference frame is chosen for convenience perpendicular to the

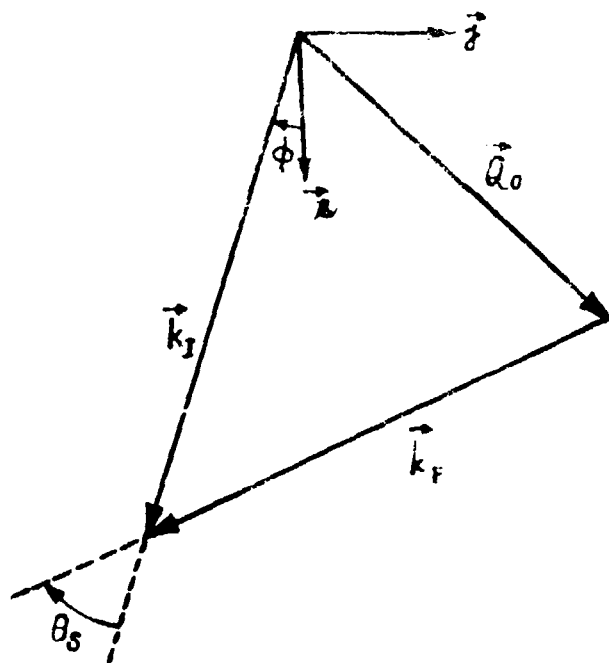


Fig. 1. Vector diagram in the reciprocal space for the most probable scattering process.

tions only elastic or at the most quasielastic scattering processes are considered. In fig. 1 there is shown a vector diagram in the reciprocal space corresponding to the most probable scattering process. The \vec{k} -axis of the rectangular reference frame is chosen for convenience perpendicular to the

plane of experiment defined by \vec{k}_I and \vec{k}_F . The orientation of \vec{i} -axis is arbitrary; for a given physical situation it may be particularised in a suitable mode.

Taking use of the measuring angles convention, described in table 2, \vec{k}_I , \vec{k}_F , \vec{k}_1 and \vec{k}_2 may be written as follows :

$$\begin{aligned} \vec{k}_I &= k_I \cos \phi \vec{i} + k_I \sin \phi \vec{j} \\ \vec{k}_F &= k_F \cos (\phi + \theta_s) \vec{i} + k_F \sin (\phi + \theta_s) \vec{j} \\ \vec{k}_1 &= k_1 \cos (\phi + \theta_s) \cos \delta_1 \vec{i} + k_1 \sin (\phi + \theta_s) \cos \delta_1 \vec{j} + k_1 \sin \delta_1 \vec{k} \\ \vec{k}_2 &= k_2 \cos (\phi + \theta_s + \theta_2) \cos \delta_2 \vec{i} + k_2 \sin (\phi + \theta_s + \theta_2) \cos \delta_2 \vec{j} + k_2 \sin \delta_2 \vec{k} \end{aligned} \quad (2)$$

Table 2

measuring angles convention

Angle	Range	Origin	Positive sense
ϕ	$[-\pi, \pi]$	The most probable \vec{k}	Trigonometrical
$\theta_s, 2\theta_M$	$[-\pi, \pi]$	The most probable \vec{k} incident.	Trigonometrical
δ	$[-\pi, \pi]$	\vec{i} -axis	Trigonometrical
δ	$[-\frac{\pi}{2}, +\frac{\pi}{2}]$	Projections of \vec{k} on the experimental plane	k_z positive

The monochromator and analyser transmission functions are expressed in simple forms in terms of k_1 , k_F , δ_1 , δ_2 , δ_1 and δ_2 variables. Thus:

$$\begin{aligned} T_M(\vec{k}_1, \vec{k}_I) &= T_{MH}(k_1, \delta_1) T_{MV}(\delta_1) \\ T_A(\vec{k}_F) &= T_{AH}(\delta_2) T_{AV}(\delta_2) \end{aligned} \quad (3)$$

where :

T_{MH} is the horizontal transmission function of the monochromator

(Cooper & Nathans, 1957):

$$T_{MH}(\delta_1, \delta_2) = P_M \exp \left\{ - \left[\frac{1}{2\alpha_c^2} (\delta_1 + 2 \frac{k_i - k_f}{k_I} \text{tg} \theta_M)^2 + \frac{1}{2\eta^2} (\delta_1 + \frac{k_i - k_f}{k_I} \text{tg} \theta_M)^2 + \frac{\delta_1^2}{2\alpha_c^2} \right] \right\} \quad (4)$$

P_M is the monochromator crystal reflectivity for the most probable neutrons.

T_{MV} is the vertical transmission function of the monochromator (Dorner, 1972; Grabcev, 1972):

$$T_{MV}(\delta_1) = \frac{\beta_c}{(\beta_c^2 + \eta^2 \sin^2 \theta_M)^{1/2}} e^{-\delta_1^2 \left[\frac{1}{2\beta_c^2 + 2\eta^2 \sin^2 \theta_M} + \frac{1}{2\beta_c^2} \right]} \quad (5)$$

T_{AH} and T_{AV} are the horizontal and vertical transmission functions of the analyser:

$$\begin{aligned} T_{AH}(\delta_2) &= e^{-\frac{\delta_2^2}{2\beta_c^2}} \\ T_{AV}(\delta_2) &= e^{-\frac{\delta_2^2}{2\beta_c^2}} \end{aligned} \quad (6)$$

For the actual values of the collimation angles and of the monochromator mosaic spread, the transmission functions (4)-(6) are sensibly different from zero only when $\delta_1, \delta_2, \delta_1$ and δ_2 do not exceed one-two degrees and $|k_i - k_f|/k_I \ll 1$. On the other hand, for quasielastic cross sections, in special experimental conditions (which will be discussed later in more detail), the wave vector length distribution in the scattered neutron beam takes essentially non-zero values only if $|k_f - k_I|/k_I \ll 1$. Under these circumstances:

- a) The small angle approximation may be used for δ and δ .
- b) The slowly varying functions of k_i and k_f may be replaced by their values in k_I .

c) All the integration limits in the expression obtained from eq.(1) replacing the variables \vec{k}_1 and \vec{k}_F by $k_1, k_F, \gamma_1, \gamma_2, \delta_1$ and δ_2 may be extended from $(0, +\infty)$, $(-\pi, +\pi)$ and $(-\pi/2, +\pi/2)$ to $(-\infty, +\infty)$ without introducing an appreciable error in the value of the integral.

Then, from eq.(1) one obtains:

$$I(\vec{k}_I, \theta_S) = \Phi(\vec{k}_I) \varepsilon(k_I) \frac{\hbar J_1}{m k_I} \int s(k_1, k_F, \gamma_1, \gamma_2, \delta_1, \delta_2) T_{MH}(k_1, \gamma_1) T_{MV}(\delta_1) \times \\ \times T_{AH}(\gamma_2) \cdot T_{AV}(\delta_2) dk_1 dk_F d\gamma_1 d\gamma_2 d\delta_1 d\delta_2 \quad (7)$$

where:

$$s = \frac{v_m k_I}{k} \frac{d\sigma}{d\vec{k}_F} = \hbar^2 \frac{d^2\sigma}{d\Omega dE_F} \quad (8)$$

and J_1 is the Jacobian of the variables transformation :

$$J_1 = \left| \frac{\partial(\vec{k}_1, \vec{k}_F)}{\partial(k_1, k_F, \gamma_1, \gamma_2, \delta_1, \delta_2)} \right| = k_1^2 k_F^2 \cos \delta_1 \cos \delta_2 \approx k_I^4 \quad (9)$$

Introducing the more convenient notation :

$$u_1 = \frac{k_1 - k_I}{k_I} \operatorname{tg} \theta_M \quad (10)$$

$$u_2 = k_F - k_I ,$$

there results the following expression of the counting rate :

$$I(\vec{k}_I, \theta_S) = \Phi(\vec{k}_I) \varepsilon(k_I) \frac{\hbar k_I^4}{m |\operatorname{tg} \theta_M|} \int s(u_1, u_2, \gamma_1, \gamma_2, \delta_1, \delta_2) T_{MH}(u_1, \gamma_1) \times \\ \times T_{MV}(\delta_1) T_{AH}(\gamma_2) T_{AV}(\delta_2) du_1 du_2 d\gamma_1 d\gamma_2 d\delta_1 d\delta_2 \quad (11)$$

Formula (11) will be used in the next sections for the derivation of the resolution function.

iv. Resolution function in the four-dimensional (\vec{Q}, ω) space.

Generally, the scattering cross sections of anisotropic systems are expressed in terms of momentum and energy transfers. However, the spread of \vec{k}_i and \vec{k}_p around \vec{k}_i and \vec{k}_p , caused by finite collimation and mosaic structure of the monochromator, leads on to a subsequent spread of momentum - and energy transfer :

$$\begin{aligned} \Delta Q &= \hbar(\vec{k}_i - \vec{k}_p) \\ \Delta \omega &= \frac{\hbar^2}{2m}(\vec{k}_i^2 - \vec{k}_p^2) \end{aligned} \quad (12)$$

around their most probable values :

$$\begin{aligned} \vec{Q}_0 &= \hbar(\vec{k}_i - \vec{k}_p) \\ \omega_0 &= \frac{\hbar^2}{2m}(\vec{k}_i^2 - \vec{k}_p^2) = 0 \end{aligned} \quad (13)$$

It is convenient to use instead of \vec{Q} and ω , their deviations from \vec{Q}_0 and ω_0 : \vec{X} and ϵ :

$$\begin{aligned} \vec{X} &= \vec{Q} - \vec{Q}_0 \\ \epsilon &= \omega - \omega_0 = 0 \end{aligned} \quad (14)$$

The four variables defined in eqs(14) are introduced in eq. (11) to replace u_2, δ_1, δ_2 and ϵ_1 ; u_1 and ϵ_2 are kept on.

Then, the counting rate becomes :

$$I(\vec{k}_I, \theta_s) = I(\vec{Q}_0) = \bar{P}(\vec{k}_I) \delta(k_I) \frac{\hbar^4 k_I^4 J_2}{m |t_{SM}|} \int s(\vec{Q}_0 + \vec{X}, X_4) T_M T_A du_1 d\delta_1 d\vec{X} dX_4 \quad (15)$$

where :

$$J_2 = \left| \frac{\partial(u_2, \delta_1, \delta_2, \epsilon_2)}{\partial(X, X_4)} \right| = \frac{m}{\hbar k_I^3 \cos \epsilon_2 \cos \delta_1 |\sin(\theta_s + \delta_2 - \delta_1)|} \frac{m}{\hbar k_I^4 |\sin(\theta_s + \delta_1)|}$$

When the scattering angles are much larger than the collimation angles (i.e. the small angle scattering is excluded) :

$$J_2 = \frac{h}{k_I \lambda \sin \theta_s} \quad (15)$$

and:

$$\begin{aligned} \delta_1 &= A_{10}u_1 + A_{11}X_1 + A_{12}X_2 + A_{14}X_4 \\ \delta_2 &= A_{20}u_2 + A_{21}X_1 + A_{22}X_2 + A_{24}X_4 \\ u_2 &= A_{30}u_1 + A_{31}X_1 + A_{32}X_2 + A_{34}X_4 \end{aligned} \quad (17)$$

$$\delta_2 = \delta_1 - \frac{1}{k_I} X_3 \quad (18)$$

where :

$$\begin{aligned} A_{10} &= \frac{\operatorname{tg} \frac{\theta_s}{2}}{\operatorname{tg} \theta_M} & A_{11} &= \frac{\cos(\phi + \theta_s)}{k_I \sin \theta_s} \\ A_{12} &= \frac{\sin(\phi + \theta_s)}{k_I \sin \theta_s} & A_{14} &= \frac{-(m/h)}{k_I^2 \sin \theta_s} \\ A_{20} &= -A_{10} & A_{21} &= \frac{\cos \phi}{k_I \sin \theta_s} \\ A_{22} &= \frac{\sin \phi}{k_I \sin \theta_s} & A_{24} &= \frac{-(m/h) \cos \theta_s}{k_I^2 \sin \theta_s} \\ A_{30} &= \frac{k_I}{\operatorname{tg} \theta_M} & A_{31} &= A_{32} = 0 & A_{34} &= \frac{-(m/h)}{k_I} \end{aligned} \quad (19)$$

Finally, the counting rate may be written as :

$$I(\vec{Q}_0) = I(\vec{k}_I) \xi(k_I) \int R(\vec{Q}_0 + \vec{k}, X_4) R(\vec{Q}_0, \vec{k}, X_4) d\vec{k} dX_4 \quad (20)$$

where :

$$R(\vec{Q}_0, \vec{k}, X_4) = \frac{1}{|\sin \theta_s \operatorname{tg} \theta_M|} \int T_M T_A du_1 d\delta_1 \quad (21)$$

is the resolution function.

In this definition, the resolution function is a dimensionless quantity, expressing the relative sensitivity of the instrument for a scattering process characterized by $\hbar(\vec{Q}_0 + \vec{X})$ and $\hbar\vec{X}_4$ momentum and energy transfers, when the diffractometer nominal setting corresponds to $\hbar\vec{Q}_0$ momentum transfer and the most probable process is an elastic one.

The explicit analytical expression of $R(\vec{Q}_0, \vec{X}, X_4)$ is obtained introducing in (21) the variables \vec{X} and X_4 by means of eqs.(17) and (18)

By virtue of relations (3), (17) and (18), R may be separated into two components :

$$R(\vec{Q}_0, \vec{X}, X_4) = R_H(\vec{Q}_0, X_1, X_2, X_4) R_V(\vec{Q}_0, X_3), \quad (22)$$

R_H and R_V being given by :

$$R_H = \frac{1}{|\sin \theta_s \operatorname{tg} \theta_M|} \int T_{MH} T_{AH} du_1 \quad (23)$$

$$R_V = \int T_{MV} T_{AV} d\delta_1 \quad (23')$$

For the description of R_H , the horizontal component of the resolution function, obtained from eq.(23) by integration, some new definitions are introduced :

$$\frac{1}{2\alpha_0^2} = m_1 \quad \frac{1}{2\eta_M^2} = m_2 \quad \frac{1}{2\alpha_1^2} = m_3 \quad \frac{1}{2\alpha_2^2} = a_1$$

$$M = m_1 m_2 + 4m_1 m_3 + m_2 m_3$$

$$S_1 = (A_{10}+2)^2 m_1 + (A_{10}+1)^2 m_2 + A_{10}^2 (m_3 + a_1) \quad (24)$$

$$T_1(n) = A_{10}(A_{11}+A_{21}) + (3-n) A_{21}$$

Then:

$$R_H(\vec{Q}_0, X_1, X_2, X_4) = R_{HO}(\vec{Q}_0) \cdot e^{-\frac{1}{2} \sum_{j=1}^3 M_{1j} X_j^2} \quad (25)$$

where :

$$R_{HO} = \frac{R_M}{|\sin \theta_2 \cos \theta_3|} \sqrt{\frac{1}{\sigma_1}} \quad (26)$$

and :

$$M_{ij} = \frac{2}{S_1} \int_{-\infty}^{\infty} M_{ij}(A_1, A_2) \cdot a_1 \int_{-\infty}^{\infty} U_1(n) U_2(n) e^{-n^2} \quad (27)$$

Using the notation :

$$\frac{1}{2\sigma_2^2} = V_1 \quad \frac{1}{2\sigma_3^2} = V_2 \quad (28)$$

$$\frac{1}{2\sigma_0^2 + 8N^2 \sin^2 \theta_M} = V_3 \quad \frac{1}{2\sigma_2^2} = V_2$$

from eq.(23') there results the vertical component of the resolution function :

$$R_V = R_{VO} e^{-\frac{1}{2} \sum_{i,j=1}^3 V_{ij} X_i^2 X_j^2} \quad (29)$$

in which :

$$R_{VO} = \sqrt{\frac{\pi \sigma_1}{S_1 (\sigma_2 + \sigma_3 + V_1)}} \quad (30)$$

and :

$$M_{33} = \frac{2}{K_1} \frac{V_1 (\sigma_2 + \sigma_3)}{\sigma_2 + V_3 + V_1} \quad (31)$$

Finally, R may be written as :

$$R(\vec{Q}_0, \vec{X}, X_4) = R_0(\vec{Q}_0) e^{-\frac{1}{2} \sum_{i,j=1}^3 M_{ij} X_i X_j} \quad (32)$$

where :

$$R_0 = R_{HO} R_{VO} \quad (33)$$

$$M_{ij} = M_{ji} \quad (34)$$

and

$$M_{13} = M_{23} = M_{43} = 0$$

Defining the "elastic" resolution function as :

$$R(\vec{Q}_0, \vec{X}) = R_0(\vec{Q}_0) e^{-\frac{1}{2} \sum_{i=1}^3 M_{ij} X_i^2} \quad (35)$$

the counting rate takes the following form :

$$I(\vec{Q}_0) = \bar{\Phi}(\vec{k}_I) \bar{\varepsilon}(\vec{k}_I) \int (\vec{Q}_0, \vec{X}) R(\vec{Q}_0, \vec{X}) d\vec{X} \quad (36)$$

where :

$$f(\vec{Q}_0, \vec{X}) = \int s(\vec{Q}_0 + \vec{X}, X_4) e^{-\frac{1}{2} M_{44} X_4^2 - (M_{14} X_1 + M_{24} X_2) X_4} dX_4 \quad (37)$$

When the scattering cross section is purely elastic

$$f = s \frac{Q_4}{Q_0} \quad (38)$$

4. Resolution function in the two-dimensional (Q, S) space

The cross section of an isotropic sample is expressed with respect to only two variables: the magnitude of the momentum transfer and the energy transfer. In this case it is convenient to define a corresponding resolution function depending as well on these variables.

Similarly to the previous case the deviations from the nominal values are used:

$$X_1 = Q - Q_0$$

$$X_2 = S - S_0 \quad (39)$$

When i-axis of the reference frame from fig.1 is directed along \vec{Q}_0 :

$$X = \frac{Q^2 - Q_0^2}{Q + Q_0} = X_1 + \frac{X_1^2 + X_2^2 + X_3^2}{2Q_0} = X_1 \quad (40)$$

Then, for an isotropic sample, from eqs.(20), (32) and (40) one obtains :

$$I(\vec{Q}_0) = \int \phi(\vec{k}_I) \varepsilon(k_I) \int s(Q_0 + X_1, X_4) R_0(\vec{Q}_0) e^{-\frac{1}{2} \sum_{j=1}^4 M_{1j} X_1 X_j} dX_2 dX_3 dX_4 \quad (41)$$

Integration in eq.(41) over X_2 and X_3 gives :

$$I(\vec{Q}_0) = \int \phi(\vec{k}_I) \varepsilon(k_I) \int s(Q_0 + X_1, X_4) R(Q_0, X_1, X_4) dX_1 dX_4 \quad (42)$$

where :

$$R(Q_0, X_1, X_4) = \frac{R_0}{4\pi k_I^2} \int e^{-\frac{1}{2} \sum_{j=1}^4 M_{1j} X_1 X_j} dX_2 dX_3 = \quad (43)$$

$$= R_0(Q_0) \cdot \frac{1}{2} (\mathcal{M}_{11} X_1^2 + 2\mathcal{M}_{14} X_1 X_4 + \mathcal{M}_{44} X_4^2) \quad (43')$$

is the resolution function in the (Q, ω) space.

From eqs.(43) and (43') there results :

$$\begin{aligned} R_0 &= \frac{R_0}{2k_I^2 \sqrt{M_{22} M_{33}}} & \mathcal{M}_{14} &= M_{14} - \frac{M_{12} M_{24}}{M_{22}} \\ \mathcal{M}_{11} &= M_{11} - \frac{M_{12}^2}{M_{22}} & \mathcal{M}_{44} &= M_{44} - \frac{M_{24}^2}{M_{22}} \end{aligned} \quad (44)$$

In order to define and in this case the resolution function as a dimensionless quantity, the k -density of the neutron flux, $\hat{\phi}(\vec{k}_I)$:

$$\hat{\phi}(\vec{k}_I) = 4\pi k_I^2 \phi(\vec{k}_I) \quad (45)$$

was introduced to replace $\phi(\vec{k}_I)$ in eq.(41).

Therefore, the resolution function in (Q, ω) space is related by means of eqs.(44) with the one, already known, defined in (\vec{Q}, ω) space. However, due to the large number of terms in M_{1j} it is difficult to obtain in this way formulae expressing in the most simple manner the resolution function dependence on experimental factors. To do so, it is preferable to reformulate the problem of the resolution function adequate to the new physical situation.

The procedure of the resolution function calculation is similar to that used in the previous section for the derivation of $R(Q_0)$. Thus Y_1 and X_2 defined, in eqs.(39) and (40), are introduced in (11) to replace two variables, say y_1 and u_2 . From eqs.(17) and (19) one finds

$$Y_1 = y_2 + B_{10}u_1 + B_{11}X_1 + B_{14}X_4 \quad (45)$$

$$u_2 = B_{30}u_1 + B_{31}X_1 + B_{34}X_4$$

where

$$B_{10} = 2A_{10} = 2 \frac{\text{tg } \frac{\theta_s}{2}}{\text{tg } \theta_M}$$

$$B_{11} = A_{11} - A_{21} = \frac{-\text{sign}(\theta_s)}{k_I \cos \frac{\theta_s}{2}} \quad (47)$$

$$B_{14} = A_{14} - A_{24} = \frac{-(m/h_I)}{k_I} \text{tg } \frac{\theta_s}{2}$$

$$B_{30} = A_{30} = \frac{1}{\text{tg } \theta_I}$$

$$B_{31} = A_{31} = 0$$

$$B_{34} = A_{34} = \frac{-\text{sign}(\theta_s)}{k_I}$$

Then, there results the following expression of the counting rate

$$I(Q_0) = \int_{\vec{k}_I} \delta(k_I) \frac{\pi k_I^4 J_2}{m |\text{tg } \theta_M|} \int \delta(Q_0, X_1, X_4) T_{MA}^T dx_1 dx_4 du_1 d^3 y_2 d\delta_1 d\delta_2 \quad (48)$$

where

$$J_3 = \left| \frac{\partial(Y_1, u_2)}{\partial(X_1, X_4)} \right| = \frac{m}{\pi k_I^2 |\cos \frac{\theta_s}{2}|} \quad (49)$$

Consequently, according to eq.(42), the resolution function may be expressed as follows

$$R(q_0, X_1, X_2) = \frac{1}{4\pi \sqrt{\cos \theta_M \cos \frac{\theta_S}{2}}} \int \frac{1}{M} \bar{I}_A d\omega_1 d\omega_2 d\omega_3 d\omega_4 \quad (50)$$

After integration in (50) one obtains the demanded expression of the resolution function, in which:

$$R_0(q_0) = \frac{\pi \bar{I}_M}{4 \sqrt{\cos \theta_M \cos \frac{\theta_S}{2}} \sqrt{S_2}} \sqrt{\frac{V_2}{V_1 V_2 (S_2 + V_2)}} \quad (51)$$

$$M_{ij} = 2M a_1 \frac{B_{1i} E_{1j}}{S_2} \quad (51')$$

and:

$$S_2 = M + a_1 \left[(B_{10} + 2)^2 m_1 + (B_{10} + 1)^2 m_2 + B_{10}^2 m_3 \right] \quad (52)$$

The "elastic" resolution function is now given by:

$$R(q_0, X_1) = R_0(q_0) = \frac{1}{2} M_{11} X_1^2 \quad (53)$$

Finally, the counting rate becomes:

$$I(q_0) = \Phi(k_T) \mathcal{E}(k_T) \int R(q_0, X_1) R(q_0, X_1) dX_1 \quad (54)$$

whereas:

$$R(q_0, X_1) = \int R(q_0, X_1, X_2) = \frac{1}{2} M_{44} X_4^2 + M_{11} X_1^2 \quad (55)$$

5. Discussion.

The results of the previous sections enable the calculation of widths and intensities in any experimental situation as well as the attempts to find how the instrumental parameters (incident neutron energy, collimations, monochromator crystal) should be changed in order to give more advantageous experimental conditions.

The validity of the present treatment is limited to the cases of elastic and quasielastic scattering cross sections which, as a matter

of fact, represent the efficiency range of the two-axis analysis. Moreover, in the latter case the due precautions must be taken to make sure that in the scattered beam the neutron energy distribution represents a narrow band around E_T . This requirement may be achieved by a suitable choice of instrumental parameters. For instance, if the scattering cross section is a Lorentzian with half width ΔE :

$$\frac{d^2\sigma}{d\Omega dE_f}(E_i, E_f) \sim \frac{(\Delta E)^2}{(\Delta E)^2 + (E_i - E_f)^2} \quad (56)$$

the half width of the neutron energy distribution in the incoming beam:

$$\Delta E_i = \frac{E_i}{\gamma} \left\{ \text{erfc}^{-1} \left(\ln 2 \frac{E_i + E_f + m_3}{E_i} \right) \right\}^{1/2} \quad (57)$$

must be chosen to a value so that the convolution of the cross section with the incident neutron intensity:

$$I(E_i) = J(E_i) e^{-\lambda^2 \frac{(E_i - E_T)^2}{(\Delta E_i)^2}} \quad (58)$$

be sufficiently narrow. The half width of the convolution of a Lorentzian with a Gaussian has been calculated by Teutsch (1971). When $\Delta E_i \ll \Delta E$, e.g., the half width of the convolution is smaller than $\sim 1.6\Delta E_i$. If necessary, more severe restrictions may be imposed to the ratio $\Delta E_i / \Delta E$ through eq.(57).

In quasielastic experiments (critical scattering with $\vec{Q} \neq 0$, quasielastic scattering in liquids, e.g.) the explicit energy dependence of the resolution function permits to take into account the inelastic effects in the interpretation of angular distribution data.

II. ANALYSIS OF THE ELASTIC COHERENT NEUTRON SCATTERING IN CRYSTALS

The resolution function of a neutron two-axis spectrometer derived in a previous paper, is used for the calculation of the widths and integrated intensities of Bragg peaks of perfect and mosaic imperfect single crystals as well as of polycrystals.

1. Introduction

In a previous paper (Grabcev, 1973) which we shall refer as paper I, the quasielastic resolution function of a neutron crystal diffractometer has been derived. The results are applied here to the analysis of the elastic coherent scattering of neutrons in crystals in the absence of multiple scattering effects. The cases of the perfect and imperfect single crystals as well as of the polycrystals are separately examined.

The use of experimental Bragg profile measurements in determining the elastic resolution function of the diffractometer as well as the explicit dependence of the various scans on instrumental parameters are closely reconsidered. To the previous results of Caglioti, Paoletti and Ricci (Caglioti, Paoletti & Ricci, 1958, 1960; Caglioti & Ricci, 1962) and of Cooper and Nathans (Cooper & Nathans, 1968 b; Cooper, 1968) there is added the calculation of the absolute

$$\begin{aligned} \frac{jG_{m_1}}{A_{12}} &= \frac{(2\pi)^3 |F(2\theta)|^2}{2V_c \pi \eta_s \eta'_s} \int \delta(Q_1 - 2\pi\epsilon) \delta(Q_2 + 2\pi\epsilon\eta_s) \delta(Q_3 + 2\pi\epsilon\eta'_s) e^{-\frac{y^2}{2\eta_s^2} - \frac{y'^2}{2\eta'^2_s}} dy' d\epsilon \\ &= \frac{|F(2\theta)|^2}{V_c^2 \sigma^2 \eta_s \eta'_s} e^{-\frac{Q_2^2}{8\pi^2 \sigma^2 \eta_s^2} - \frac{Q_3^2}{8\pi^2 \sigma^2 \eta'^2_s}} \delta(Q_1 - 2\pi\epsilon) \end{aligned} \quad (35)$$

The counting rate describing the corresponding Bragg peak is obtained introducing eq. (35) into eq.(36) of paper I. There results:

$$I(\theta_s) = I(\theta_B) e^{-\frac{1}{2} (M'_{11} q_1^2 + 2M'_{12} q_1 q_2 + M'_{22} q_2^2 + M'_{33} q_3^2)} \quad (36)$$

where:

$$I'(\theta_s) = \frac{I(\theta_B)}{\sqrt{(4k_s^2 \sin^2 \theta_B \eta_s^2 M_{12} + 1)(4k_s^2 \sin^2 \theta_B \eta'_s M_{33} + 1)}} = \frac{I(\theta_B)}{\sqrt{(2\eta_s^2 \frac{l_{12}}{s_1} + 1)(2\eta'^2_s l_{33} + 1)}} \quad (37)$$

$$M'_{11} = M_{11} - \frac{4k_s^2 \sin^2 \theta_B \eta_s^2 M_{12}^2}{4k_s^2 \sin^2 \theta_B \eta_s^2 M_{12} + 1} = \frac{l'_{11}}{2S_1 k_s^2 \cos^2 \theta_B}; \quad l'_{11} = \frac{8\eta_s^2 a_1 M + l_{11}}{\frac{2\eta_s^2 l_{12}}{s_1} + 1}$$

$$M'_{12} = \frac{M_{12}}{4k_s^2 \sin^2 \theta_B \eta_s^2 M_{12} + 1} = \frac{l'_{12}}{2S_1 k_s^2 \sin \theta_B \cos \theta_B}; \quad l'_{12} = \frac{l_{12}}{\frac{2\eta_s^2 l_{12}}{s_1} + 1}$$

$$M'_{22} = \frac{M_{22}}{4k_s^2 \sin^2 \theta_B \eta_s^2 M_{12} + 1} = \frac{l'_{22}}{2S_1 k_s^2 \sin^2 \theta_B}; \quad l'_{22} = \frac{l_{22}}{\frac{2\eta_s^2 l_{22}}{s_1} + 1} \quad (38)$$

$$M'_{33} = \frac{M_{33}}{4k_s^2 \sin^2 \theta_B \eta'^2_s M_{33} + 1} = \frac{l'_{33}}{2k_s^2 \sin^2 \theta_B}; \quad l'_{33} = \frac{l_{33}}{2\eta'^2_s l_{33} + 1}$$

Therefore, the profile of Bragg peaks of a mosaic imperfect single crystal are determined by the resolution function of the diffractometer as well as by the mosaic spread of the sample. They are given by the same formulae as in the case of the perfect crystal in which $I(\theta_B)$, M_{ij} and l_{ij} are replaced by $I'(\theta_B)$, M'_{ij} and l'_{ij} , respectively. The half widths at half maximum as well as the integrated intensities of Bragg peaks of a mosaic crystal, corresponding to some particular scans, are listed in Table 1.

Table 1. The half widths and integrated intensities of Bragg peaks of a mosaic crystal.

Scan	Definition	Scale	(Half width) ²	(Integrated intensity) ² / C ₀
(y)	x = z = 0	y	$L_y^2 = \ln 2 \left(\frac{\beta_1}{C_0} + 2\eta_1^2 \right)$ $= L_y^1 + L_{y0}^2$	$\frac{1}{2\alpha} \frac{\omega_2}{\omega_1 (\omega_2 + \omega_3 + \sqrt{\omega_1})} (2\eta_1^2 (C_0 + 1))$
(y, -2y)	x = -2y z = 0	y	$L_{y-2y}^2 = \ln 2 \frac{\beta_1 + 2\eta_1^2 C_0}{C_0 + 8\eta_1^2 \omega_1 M}$ $= L_{y-2y}^1 - \frac{1 + L_{y0}^2 / L_y^2}{1 + 4L_{y0}^2 / L_y^2} \frac{C_0 M}{(C_0 + 1)}$	$\frac{\omega_3}{C_0 + 8\eta_1^2 \omega_1 M} \omega_1 (\omega_2 + \omega_3 + \sqrt{\omega_1}) (2\eta_1^2 (C_0 + 1))$
(x)	y = z = 0	$\frac{x}{2}$	$L_{\frac{x}{2}}^2 = \ln 2 \frac{\beta_1 + 2\eta_1^2 C_0}{4\omega_1 (C_0 + 1) + 8\eta_1^2 \omega_1 M}$ $= L_{\frac{x}{2}}^1 - \frac{1 + L_{x0}^2 / L_{\frac{x}{2}}^2}{1 + 4L_{x0}^2 / L_{\frac{x}{2}}^2} \frac{C_0 M}{(C_0 + 1)}$	$\frac{1}{4\omega_1 (C_0 + 1) + 8\eta_1^2 \omega_1 M} \omega_1 (\omega_2 + \omega_3 + \sqrt{\omega_1}) (2\eta_1^2 (C_0 + 1))$
(z)	y = x = 0	z	$L_z^2 = \ln 2 \left(\frac{1}{C_0} + 2\eta_1^2 \right)$ $= L_z^1 + L_{z0}^2$	$\frac{1}{C_0 \left(\frac{2\eta_1^2 C_0}{C_0} + 1 \right)} \omega_1 (\omega_2 + \omega_3 + \sqrt{\omega_1})$

$$R_c = \frac{\pi R}{k_I \cos \theta_B \sqrt{V_1}} \sqrt{\frac{v_2}{v_2 V_1 (v_2 + v_3)}} \quad (45)$$

$$k_I = \frac{2 M a_1}{k_I^2 \cos^2 \theta_B a_2}$$

Therefore, the Bragg peak is described by:

$$I(x) = I_p(\theta_B) e^{-\frac{C a_1}{a_2} x^2} \quad (46)$$

where $I_p(\theta_B)$ represents the maximum intensity:

$$I_p(\theta_B) = \frac{C_p}{\sqrt{\pi} \epsilon_{11}} \sqrt{\frac{v_2}{v_2 V_1 (v_2 + v_3)}} \quad (47)$$

C_p is a proportionality factor:

$$C_p = (\pi \sqrt{\pi})^3 \Phi(\vec{Q}) \epsilon(\vec{Q}) V \frac{v_2 |F(2\pi\vec{Q})|^2 \rho_1}{v_2^2 |x \cos \theta_B \sin \theta_B| |y \sin \theta_B|} = \frac{v_2 C_3}{8 |x \sin \theta_B|} \quad (48)$$

Consequently, in the x -scale, the half widths and the integrated intensities of Bragg peaks of a polycrystal are given by:

$$\Delta x = \sqrt{\frac{k_{12} k_{22}}{M}} \quad (49)$$

$$J_x = \frac{C_p}{\sqrt{M} a_1} \sqrt{\frac{v_2}{v_2 V_1 (v_2 + v_3)}}$$

When the Q -units are used (scale factor $k_I \cos \theta_B$):

$$L_x = k_I \cos \theta_B \Delta x \quad (50)$$

$$I_x = k_I \cos \theta_B J_x$$

5. Discussion.

By a proper choice of the reference frame, the equiintensity ellipsoids are directly visualized in the reciprocal lattice of the sample. The eq. (11) enables the calculation of the width and integrated intensity for any scan. However, in the paper only straight-line scans have been considered, there being no an evident advantage for a scan whose trajectory in \vec{Q} space is a more or less complicated curve.

The expressions of half widths and integrated intensities

values of intensities and of their dependence on vertical resolution.

2. Perfect single crystal

The equation of the diffraction pattern of a perfect single crystal is obtained introducing in eq. (36) of paper I the elastic coherent scattering cross section (Cassels, 1950):

$$\frac{d\sigma}{d\Omega} = \frac{Q\pi^2}{V_c} |F(\vec{Q})|^2 \sum_{\vec{G}} \delta(\vec{Q} + \sigma\vec{G}) \quad (1)$$

where:

- V_c is the volume of the unit cell,
- $F(\vec{Q})$ is the structure - including Debye-Waller factor,
- \vec{G} is any vector in the reciprocal lattice of the sample.

Therefore:

$$I(\vec{Q}) = N \frac{Q\pi^2}{V_c} |F(\vec{Q})|^2 \sum_{\vec{G}} |F(\sigma\vec{G})|^2 \delta(\vec{Q} + \sigma\vec{G}) e^{-\frac{1}{2} \sum_{\alpha} M_{\alpha} (\vec{Q} + \sigma\vec{G})^2} \quad (2)$$

that a set of peaks whose widths and intensities are essentially determined by the resolution function.

When the \vec{Q} -axis of the reference frame from Fig. 1 of paper I (in which as it was already pointed out, $Q_{0y} = 0$) is oriented directly towards a certain reciprocal vector of the sample, i.e. $\vec{Q} = \sigma\vec{G}$, the corresponding Bragg peak is described by:

$$I(\vec{Q}) = I(\theta_B) \frac{1}{2} [M_{11}(Q_{0x} - \sigma\pi)^2 + 2M_{12}(Q_{0x} - \sigma\pi)Q_{0z} + M_{22}Q_{0z}^2] \quad (3)$$

where $I(\theta_B)$ represents the peak intensity, occurring when:

$$Q_{0x} = k_z [\sin \phi - \sin(\phi + \theta_s)] = 0 \quad (4)$$

and:

$$Q_{0z} = k_z [\cos \phi - \cos(\phi + \theta_s)] = 2\pi\sigma = 2k_z |\sin \theta_s| \quad (5)$$

The condition (4) leads to:

$$\phi = \frac{\pi}{2} \operatorname{sgn}(\theta_s) - \frac{\theta_s}{2} \quad (6)$$

while (5) demands:

$$\theta_s = 2 \theta_B \quad (7)$$

The shape of the peak is dependent on scanning procedure.

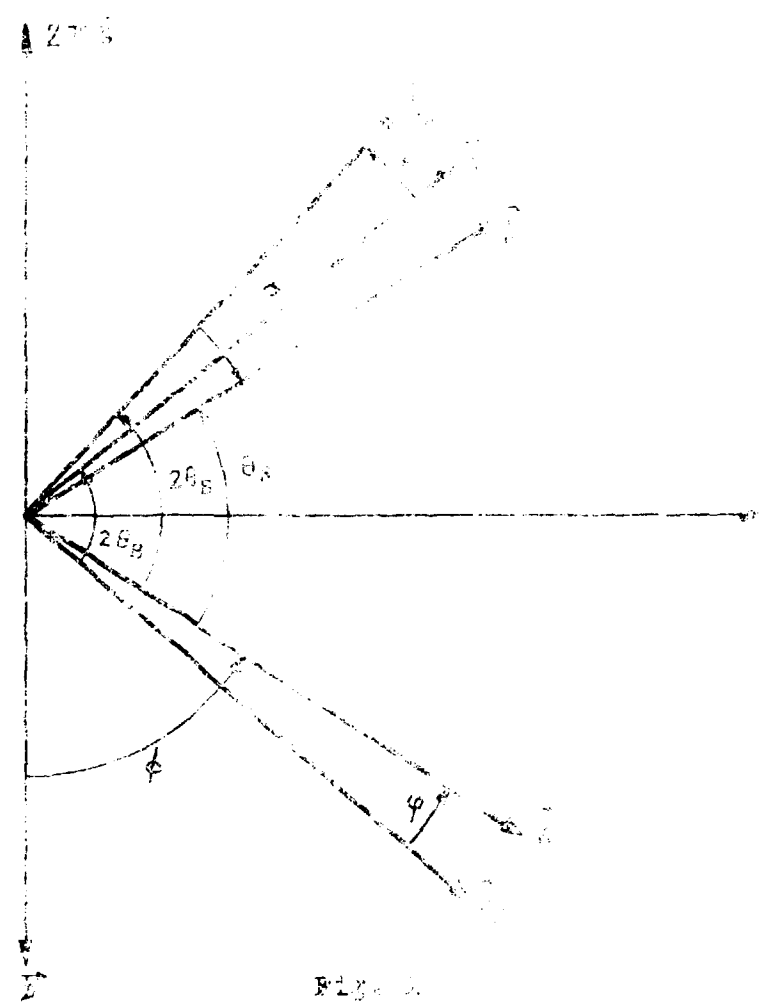


Fig. 1

Diagram in the horizontal plane illustrating the relationship between missing angles and the most probable wave vectors.

In our particular reference frame \vec{Q}_1 may be changed rotating \vec{E}_p about a vertical axis. The rotation of the semole through an angle $-\varphi$ from the optimum position (Fig. 1) is equivalent to the rotation both \vec{k}_I and \vec{k}_p through an angle φ in position k_I and \vec{k}_p' , the scattering angle remaining equal to $2\theta_s$. The vector rotation by an angle φ represents a rotation of \vec{E}_p through the same angle, to \vec{E}_p' . In this configuration:

$$\varphi = \frac{\pi}{2} (\theta_p - \theta_s) - \theta_s + \varphi$$

$$\theta_s = 2\theta_p - \varphi$$

and consequently:

$$\begin{aligned} Q_{01} - 2\pi\epsilon &= k_1 x \cos \theta_0 \\ Q_{02} &= k_1 (x + 2y) \sin \theta_0 \end{aligned} \quad (9)$$

At a rotation of the reference frame (i.e. of the sample) through a small angle Ψ (comparable with the vertical collimation angles), about \vec{j} -axis, the components of the scattering vector are changed in the following way:

$$\begin{aligned} Q'_{01} &= Q_{01} \cos \Psi \approx Q_{01} \\ Q'_{02} &= Q_{02} \\ Q'_{03} &= Q_{01} \sin \Psi \approx \Psi (2\pi\epsilon + k_1 x \cos \theta_0) \approx 2k_1 \Psi \sin \theta_0 \end{aligned} \quad (10)$$

As it may be seen in eq. (10) the horizontal component of the scattering vector is not changed when Ψ is a small quantity; the greater Ψ values are not important due to vertical collimation. Consequently, all the results obtained in paper I under the oversimplifying assumption $Q_{03} = 0$ rest valid, and the counting rate for a general configuration defined by missetting angles φ , α and Ψ is given by:

$$I(\theta_0, \vec{q}) = I(\theta_0) e^{-\frac{1}{2} (M_{11} q_1^2 + 2M_{12} q_1 q_2 + M_{22} q_2^2 + M_{33} q_3^2)} \quad (11)$$

where:

$$q_i = Q_{0i} + 2\pi \epsilon_i \quad (12)$$

In our particular reference frame, according to eqs.

$$\begin{aligned} (9) \text{ and } (10): \quad q_1 &= k_1 x \cos \theta_0 \\ q_2 &= k_1 (x + 2y) \sin \theta_0 \\ q_3 &= 2k_1 \Psi \sin \theta_0 \end{aligned} \quad (13)$$

The elements of the resolution function entering eq. (11) are given by eqs. (26), (27), (40) and (51) of paper I, which in agreement with eqs. (6) and (7) $\phi = \frac{M}{2S_1} \cos \theta_3$ and $\theta_3 = 2\theta_1$.

Hence:

$$A_{10} = -A_{20} = \frac{\text{tg } \theta_1}{\text{tg } \theta_3} \quad \text{with } a = \text{dispersion parameter (Ogilvie, Paoletti & Ricci, 1957)}$$

$$A_{11} = -A_{21} = \frac{\text{sign } (\theta_1)}{2k_T \cos \theta_3} \quad (14)$$

$$A_{12} = A_{22} = \frac{\text{sign } (\theta_1)}{2s_T \sin \theta_3}$$

$$S_1 = (a+2)^2 m_1 + (a+1)^2 m_2 + a^2 (m_3 + a_1) \quad (15)$$

$$M_{11} = \frac{l_{11}}{2S_1 k_T^2 \cos^2 \theta_3} \quad M_{22} = \frac{l_{22}}{2S_1 k_T^2 \sin^2 \theta_3} \quad (16)$$

$$M_{12} = \frac{l_{12}}{2S_1 k_T^2 \sin \theta_3 \cos \theta_3} \quad M_{33} = \frac{l_{33}}{2 k_T^2 \sin^2 \theta_3}$$

where:

$$\begin{aligned} l_{11} &= M + (4m_1 + m_2) a \\ l_{12} &= -M + \{4(a+1)m_1 + (2a+1)m_2\} a \\ l_{22} &= M + \{4(a+1)^2 m_1 + (2a+1)^2 m_2 + 4a^2 m_3\} a \end{aligned} \quad (17)$$

$$l_{33} = 4v_1 \frac{v_2 + v_3}{v_2 + v_3 + v_1} \sin^2 \theta_3$$

The following identities will be further used in expressing the peak widths and integrated intensities

$$\begin{aligned} l_{11} + 2l_{12} + l_{22} &= 4(S_1 - a^2 a_1) a_1 \\ l_{11} l_{22} - l_{12}^2 &= 4a_1 M S_1 \end{aligned} \quad (18)$$

The optimum intensity is obtained from eq. (11) when:

$$\alpha = \beta = \gamma = 0 \quad (19)$$

Hence:

$$I(\theta_B) = \Phi(\vec{k}_j) \varepsilon(k_j) \frac{N(2\pi)^3 |F|^2}{V_c^2 \sin 2\theta_B} \frac{P_m}{|t_j \theta_B|} \sqrt{\frac{\pi}{s_1}} \sqrt{\frac{\pi s_2}{s_1(s_2 + s_3 + V_4)}} \quad (19)$$

If we introduce the incoming flux of monochromatic neutrons (expressed in n.cm⁻² sec⁻¹):

$$I_0 = \int \Phi(\vec{k}_j) T_m(\vec{k}_i, k_j) d\vec{k} = \pi^{3/2} \frac{\Phi(\vec{k}_j) k_j^3 P_m}{|t_j \theta_B| \sqrt{V_c}} \sqrt{\frac{s_2}{s_1(s_2 + s_3)}} \quad (20)$$

and the crystallographic quantity Q_B (James, 1958):

$$Q_B = \frac{(2\pi)^3 |F(2\pi \vec{r})|^2}{V_c^2 \sqrt{c} \sin 2\theta_B} \quad (21)$$

the peak intensity will be given by:

$$I(\theta_B) = I_0 Q_B V \varepsilon(k_j) \sqrt{\frac{M}{\pi s_1}} \sqrt{\frac{s_2 + s_3}{s_2 + s_3 + V_4}} \quad (22)$$

where V is the sample volume.

Formula (11) indicates that the locus of points in \vec{q} space for which the counting rate is p -times smaller than in the Bragg position ($\vec{q} = 0$), is an ellipsoid:

$$M_{11} q_1^2 + 2 M_{12} q_1 q_2 + M_{22} q_2^2 + M_{33} q_3^2 = 2 p_m f \quad (23)$$

Consequently, the shape of Bragg peaks is dependent on the direction of displacement in \vec{q} space during the scan. If $q_{\xi\zeta}$, ξ and ζ are coordinates in \vec{q} space, defined by:

$$\begin{aligned} q_1 &= q_{\xi\zeta} \cos \xi \cos \zeta \\ q_2 &= q_{\xi\zeta} \sin \xi \cos \zeta \\ q_3 &= q_{\xi\zeta} \sin \zeta \end{aligned} \quad (24)$$

where according to eqs. (13):

$$\begin{aligned} q_{\xi\zeta} &= k_f \sqrt{x^2 + 4(x\gamma + \gamma^2 + \gamma^2) \sin^2 \theta_B} \\ t_j \xi &= \frac{x + 2\gamma}{x} t_j \theta_B \\ t_j \zeta &= \frac{2\gamma t_j \theta_B}{\sqrt{x^2 + (x + 2\gamma)^2 t_j^2 \theta_B^2}} \end{aligned} \quad (25)$$

the Bragg peak measured along a direction in \vec{q} space defined by the angles ξ and ζ is described by:

$$I(\theta_0, \chi_{FS}) = I(\theta_0) e^{-\frac{1}{2} M(\xi\xi) \frac{q^2}{\lambda_{FS}^2}} \quad (26)$$

where:

$$M(\xi\xi) = M_{11} \cos^2 \xi \cos^2 \zeta + 2M_{12} \cos \xi \sin \xi \cos^2 \zeta + M_{22} \sin^2 \xi \cos^2 \zeta + M_{33} \sin^2 \zeta \quad (27)$$

Therefore, the Bragg peaks are Gaussians whose integrated intensities and half widths at half maximum are given by:

$$I(\xi\xi) = \int I(\theta_0, \chi_{FS}) d\chi_{FS} = I(\theta_0) \sqrt{\frac{2\pi}{M(\xi\xi)}} \quad (28)$$

$$L(\xi\xi) = \sqrt{\frac{2 \ln 2}{M(\xi\xi)}} \quad (29)$$

Formulae (28) and (29) will be further applied to the calculation of Bragg peaks characteristics of ideal single crystals for some usual scanning procedures.

Crystal (φ) scan.

In a (φ) scan, sample crystal is rotated about a vertical axis keeping the detector fixed in the Bragg position. In this situation $\chi = \psi = 0$ and according to eqs.(25) $\xi = \pi/2$ and $\zeta = 0$. Then $q_1 = q_3 = 0$, i.e. the intensity ellipsoids are scanned along q_2 axis. Therefore:

$$I_\varphi = I(\theta_0) \sqrt{\frac{2\pi}{M_{22}}} \quad (30)$$

$$L_\varphi = \sqrt{\frac{2 \ln 2}{M_{22}}}$$

In eq. (30) I_φ and L_φ are expressed in units of q . However, usually, the Bragg peaks are plotted in terms of angular units. Eqs. (30) may be rewritten in φ -scale dividing them by a scale factor equal to $2k_1 \sin \theta_B$ (as obtained from eqs. (25)). Hence, making use of eqs. (16), the peak integrated intensity and half width in φ -scale are given by:

$$I_\varphi = I(\theta_0) \sqrt{\frac{\pi s_1}{L_{22}}} \quad (30')$$

$$L_\varphi = \sqrt{\frac{\ln 2 \cdot s_1}{L_{22}}}$$

Crystal-detector ($\psi, -2\psi$) scan.

In this scan $\chi = -2\psi$ and $\Upsilon = 0$. Then $\bar{X} = \bar{Y} = 0$ and $q_2 = q_3 = 0$, i.e. the scanning is performed along q_1 axis. Hence:

$$I_{\psi, -2\psi} = K(\theta_0) \sqrt{\frac{2\pi}{M_{11}}} \quad (31)$$

and in ψ -scale:

$$L_{\psi, -2\psi} = \sqrt{\frac{2\pi}{M_{11}}}$$

$$I_{\psi, -2\psi} = K(\theta_0) \sqrt{\frac{2\pi}{M_{11}}}$$

$$d_{\psi, -2\psi} = \sqrt{\frac{2\pi}{M_{11}}} \quad (31')$$

(the scale factor is now $2k_1 \cos \theta_0$)

Detector (χ) scan.

When the crystal is kept fixed in the Bragg position and the detector is rotated ($\psi = \Upsilon = 0$), $\bar{X} = \theta_0$ and $\bar{Y} = 0$. Then:

$$q_1 = k_1 \chi \cos \theta_0$$

$$q_2 = k_1 \chi \sin \theta_0$$

$$q_3 = 0$$

and:

$$I_{\chi} = K(\theta_0) \sqrt{\frac{2\pi}{M_{11} \cos^2 \theta_0 + 2M_{12} \cos \theta_0 \sin \theta_0 + M_{22} \sin^2 \theta_0}} \quad (32)$$

$$L_{\chi} = \sqrt{\frac{2\pi}{M_{11} \cos^2 \theta_0 + 2M_{12} \cos \theta_0 \sin \theta_0 + M_{22} \sin^2 \theta_0}}$$

In $\chi/2$ -scale (scaling factor $2k_1$):

$$I_{\chi/2} = K(\theta_0) \sqrt{\frac{2\pi}{2M_{11} + 2M_{12} \sin 2\theta_0 + M_{22} \sin^2 2\theta_0}} \quad (32')$$

$$L_{\chi/2} = \sqrt{\frac{2\pi}{2M_{11} + 2M_{12} \sin 2\theta_0 + M_{22} \sin^2 2\theta_0}}$$

Vertical (Υ) scan

If the crystal is rotated from the Bragg position about \bar{Y} -axis ($\psi = \chi = 0$), $\bar{X} = \pi/2$, i.e. the scanning is made along q_2 axis. The integrated intensity and the half width of the peak are in this case:

$$I_{\Upsilon} = K(\theta_0) \sqrt{\frac{2\pi}{M_{22}}} \quad (33)$$

$$L_{\Upsilon} = \sqrt{\frac{2\pi}{M_{22}}}$$

In Υ -scale (scaling factor $2k_2 \sin \theta_0$):

$$T_c = I(\theta_0) \sqrt{\frac{\pi}{L_{33}}}$$

$$L_{33} = \sqrt{\frac{L_{22}}{L_{11}}}$$

(33')

The M_{ij} coefficients defining in eq. (23) the equintensity ellipsoids are nothing else than the elements of the resolution matrix corresponding to Bragg position of the sample. That means, in these particular points of (Q, W) space, the resolution function of the diffractometer may be directly determined experimentally from the widths and intensities of Bragg peaks of a perfect crystal, measured in various scanning modes (Cooper & Nathans, 1968 b).

Mosaic imperfect single crystal.

The cross section of a mosaic imperfect crystal may be obtained averaging the cross section of a perfect crystal with respect to mosaic block distribution (Cooper & Nathans, 1968 a).

When a certain reciprocal vector of the most probable mosaic blocks is oriented against to \hat{i} -axis (i.e. $\vec{s} = -\tau \hat{i}$), the corresponding reciprocal vector attached to a mosaic block, described by horizontal and vertical mosaic angles φ_1 and ψ_1 , respectively, is given by:

$$\begin{aligned} \vec{s}' &= -\tau \cos \varphi_1 \cos \psi_1 \hat{i} + \tau \sin \varphi_1 \cos \psi_1 \hat{j} + \tau \sin \varphi_1 \hat{k} \\ &= -\tau \hat{i} + \tau \varphi_1 \hat{j} + \tau \psi_1 \hat{k} \end{aligned}$$

Then:

$$\frac{d\sigma_m}{d\Omega} = \int \frac{d\sigma}{d\Omega}(\tau(\varphi_1, \psi_1)) P(\varphi_1) P(\psi_1) d\varphi_1 d\psi_1 \quad (34)$$

where $P(\varphi_1)$ and $P(\psi_1)$ are the distribution functions of the mosaic angles. When they are Gaussian functions with half widths $L_{SH} = (2 \ln 2)^{1/2} \eta_S$ and $L_{SV} = (2 \ln 2)^{1/2} \eta_V$, respectively, the scattering cross section becomes:

relationships of order of preferred axes for single crystals, collection of the h and k profiles to detector scan for polycrystals, given in eqs. (1) are in agreement with those reported by Caglioti, *et al.* and also by *et al.* of Cooper and Nathans. Moreover, the determination of C_1 and C_2 proportional factors as well as of the dependence of the integrated intensities on vertical collimations and scans appears performed in the present paper, come to complete the results of the above mentioned authors.

REFERENCES I

- Caglioti, G. (1964). Acta Cryst. 17, 1202.
- Caglioti, G., Paoletti, A. & Ricci, F.P. (1958). Nucl.Instrum.Meth. 3, 220.
- Caglioti, G., Paoletti, A. & Ricci, F.P. (1960). Nucl.Instrum.Meth. 9, 195.
- Caglioti, G. & Ricci, F.P.(1962). Nucl.Instrum.Meth. 15, 155.
- Cooper, M.J.(1968), Acta Cryst. A24, 624.
- Cooper, M.J. & Nathans, R.(1967). Acta Cryst. 23, 357.
- Cooper, M.J. & Nathans, R.(1968 a). Acta Cryst. A24, 481.
- Cooper, M.J. & Nathans, R.(1968 b). Acta Cryst. A24, 619.
- Cooper, M.J.(1972). Acta Cryst. A28, 319.
- Grubcevic, B. (1972). I.F.A. , PAN.-42.
- Grubcevic, B. (1973 a). Nucl. Instrum. Meth. 106, 349.
- Grubcevic, B. (1973 b). Rev.Roum.Phys. 18. 373.
- Deutsch, H. (1971). Stud.Cerc.Fiz. 23, 517.
- Bocchiarone, A. Lau, H.Y., Corliss, L.H., Delapalme, A. & Hastings, J.H. (1971). Phys.Rev. B4, 3206.
- Hillis, B.T.M.(1960). Acta Cryst. 13, 763.

REFERENCES II

- G.Caglioti, A.Paoletti & F.P.Ricci, (1958) Nucl.Instrum.Meth.3,323.
- G.Caglioti, A.Paoletti & F.P.Ricci, (1960) Nucl.Instrum.Meth.9,195.
- G.Caglioti & F.P.Ricci, (1962) Nucl.Instrum.Meth. 15,155.
- J.M.Cassels (1950) Progr. Nucl. Phys. 1,185.
- M.J.Cooper, Acta Cryst.A24, 624.
- M.J.Cooper & R.Nathans, (1968 a). Acta Cryst. A24, 481.
- M.J.Cooper & R.Nathans, (1968 b). Acta Cryst. A24, 619.
- B.Grubcevic, (1973) Paper I
- R.V.James, (1958), "The Optical Principles of the Diffraction of X-Rays", G.Bell and Sons Ltd., London.